

Neural Collapse for Cross-entropy Class-Imbalanced Learning with Unconstrained ReLU Feature Model

Hien Dang[†] Tho Tran[†] Tan Nguyen^{*,‡‡} Nhat Ho^{*,††}

FPT Software AI Center, Vietnam[†]

Department of Statistics and Data Sciences, University of Texas at Austin, USA^{††}

Department of Mathematics, National University of Singapore, Singapore^{‡‡}

January 5, 2024

Abstract

The current paradigm of training deep neural networks for classification tasks includes minimizing the empirical risk that pushes the training loss value towards zero, even after the training error has been vanished. In this terminal phase of training, it has been observed that the last-layer features collapse to their class-means and these class-means converge to the vertices of a simplex Equiangular Tight Frame (ETF). This phenomenon is termed as Neural Collapse (\mathcal{NC}). To theoretically understand this phenomenon, recent works employ a simplified unconstrained feature model to prove that \mathcal{NC} emerges at the global solutions of the training problem. However, when the training dataset is class-imbalanced, some \mathcal{NC} properties will no longer be true. For example, the class-means geometry will skew away from the simplex ETF when the loss converges. In this paper, we generalize \mathcal{NC} to imbalanced regime for cross-entropy loss under the unconstrained ReLU feature model. We prove that, while the within-class features collapse property still holds in this setting, the class-means will converge to a structure consisting of orthogonal vectors with different lengths. Furthermore, we find that the classifier weights are aligned to the scaled and centered class-means with scaling factors depend on the number of training samples of each class, which generalizes \mathcal{NC} in the class-balanced setting. We empirically prove our results through experiments on practical architectures and dataset.

1 Introduction

Cross-entropy (CE) is undoubtedly one of the most popular loss functions to train neural networks for classification tasks in the current paradigm of deep learning. However, some key questions about training networks using this loss function have not been fully explored yet, for example: i) Is there any unique pattern that the models learn when training deep neural networks until convergence, i.e., to reach zero loss?, ii) How does the structure of the parameters vary across data distribution, training instances, and model architecture?, iii) What are the geometries of the learned representations and the classifier obtained from minimizing CE loss?. Understanding these questions is crucial for the study of the training and generalization properties of deep neural networks. For example, it has been a long-standing problem that training neural networks using CE loss under a long-tailed distribution dataset causes a significant drop in accuracy, especially for classes with a scarce amount of training samples. This phenomenon can be understood via the geometry of the learned model's classifier weight, where the weight vector of a more frequent class has a larger norm, thus the decision boundary is biased toward the less frequent class. As a consequence, a smaller volume of the feature

* Co-last authors.

space is allocated for the minority classes, which leads to a drop in performance. [14, 13, 2, 27, 17, 12].

A noticeable progress in answering these questions is the discovery of *Neural Collapse* phenomenon [20]. Neural Collapse (\mathcal{NC}) reveals a common pattern of the learned last-layer features and the classifier weight of deep neural networks across canonical datasets and architectures. Specifically, \mathcal{NC} consists of four properties emerging in the terminal phase of training (TPT) of training deep neural networks for balanced datasets (i.e., every class has the same number of training instances):

- ($\mathcal{NC1}$) **Variability collapse:** features of the samples within the same class converge to a unique vector (i.e., the *class-mean*), as training progresses.
- ($\mathcal{NC2}$) **Convergence to simplex ETF:** the optimal class-means have the same length and are equally and maximally pairwise separated, i.e., they form a simplex Equiangular Tight Frame (ETF).
- ($\mathcal{NC3}$) **Convergence to self-duality:** up to rescaling, the class-means and classifiers converge on each other.
- ($\mathcal{NC4}$) **Simplification to nearest class-center:** given a feature, the classifier converges to choosing whichever class has the nearest class-mean to it.

The intriguing empirical observation of Neural Collapse has attracted many theoretical investigations, mostly under a simplified *unconstrained feature model (UFM)* (see Section 3) and for *balanced dataset*, proving that \mathcal{NC} properties occur at any global solution of the loss function. However, under *imbalanced dataset*, it has been observed that deep neural networks exhibit different geometric structures and some \mathcal{NC} properties are not satisfied anymore. The last-layer features of samples within the same class still converge to their class-means ($\mathcal{NC1}$), but the class-means and the classifier weights will no longer form a simplex ETF ($\mathcal{NC2}$). In a more extreme case where the imbalance level is greater than some threshold, both the learned features and classifier of the minority classes will collapse on each other and become indistinguishable from those of other classes [4]. This phenomenon, named as *Minority Collapse*, explains why the accuracy for these minority classes will drop significantly compared to the balance setting.

While the \mathcal{NC} emergence in deep neural networks training using CE loss for *balanced dataset* has been extensively studied [18, 31], the similar results for *imbalanced scenario* has remained limited. Under imbalanced regime, there are several theoretical works addressed this phenomenon with the use of unconstrained feature model (UFM) for other loss functions. In particular, [3] has extensively characterized the convergence geometry for the mean squared error (MSE) loss. [22] studies the support vector machine (SVM) problem whose global minima follows a different geometry, called “SELI” and later [1] extends it to some other SVM parameterizations.

Comparison to concurrent work [8]: For CE loss, we note that the concurrent work [8] is closest to our work and [8] studies CE loss with UFM under imbalanced setting. They prove that the within-class features will collapse ($\mathcal{NC1}$) and the *network output prediction vectors converge to a block structure* where each block corresponds to a group of classes where each class has the same amount of training samples. However, since the magnitude of prediction vectors and the magnitude of each block within the structure are not yet covered, it is not yet possible to describe the geometry

explicitly and quantify how the structure changes under different imbalance levels. Furthermore, the structure of the learned last-layer feature, the classifier weight ($\mathcal{NC2}$) and the relation between them ($\mathcal{NC3}$) have not been derived in [8]. Therefore, the norm, the norm ratio, and the angle between the classifier weights and features are not considered.

On the other hand, in this paper, we study CE loss training problem using UFM, but with a slight modification, in which the features have to be *element-wise non-negative*. This setting is motivated by the current paradigm that features are typically the outcome of some non-negative activation function, like ReLU or sigmoid. In this setting, we study the global solutions of CE training problem under UFM and present a thorough analysis of the convergence geometry of the last-layer features and classifier. We summarize our contributions as follows:

- We provide the explicit characterization for the last-layer features and classifier weights of CE loss training with the use of UFM and non-negative features. We prove that at optimality, $\mathcal{NC1}$ still occurs, and the optimal class-means form an orthogonal structure. We derive the closed-form lengths of the features and classifiers, in terms of the number of training samples and other hyperparameters.
- We find that the classifier weight is aligned to a scaled and centered version of the class-means, which generalizes the property $\mathcal{NC3}$ from the original definition. Also, we derive the norms, norm ratios and angles between these classifier weights explicitly.
- We derive the exact threshold for a class to collapse and become indistinguishable from other classes. Hence, the threshold for Minority Collapse is also obtained.

Notation: For a weight matrix \mathbf{W} , we use \mathbf{w}_j to denote its j -th row vector. $\|\cdot\|_F$ denotes the Frobenius norm of a matrix and $\|\cdot\|_2$ denotes L_2 -norm of a vector. \otimes denotes the Kronecker product. The symbol “ \propto ” denotes proportional, i.e, equal up to a positive scalar. We also use some common matrix notations: $\mathbf{1}_n$ is the all-ones vector, $\text{diag}\{a_1, \dots, a_K\}$ is a square diagonal matrix size $K \times K$ with diagonal entries a_1, \dots, a_K . We use $[K]$ to denote the index set $\{1, 2, \dots, K\}$.

2 Related Works

Neural Collapse on balanced dataset: A surge of theoretical results for Neural Collapse under balanced scenario has emerged after the discovery of this phenomenon [18, 31, 5, 29, 30, 23, 3, 22, 1, 15]. Due to the highly non-convexity of the problem of training deep networks, theoretical works have proven the occurrence of \mathcal{NC} for different loss functions and architectures with a simplified unconstrained features model (see Section 3 for more details). In particular, \mathcal{NC} properties are proven to occur to the last-layer features and classifier across different loss functions: cross-entropy [18, 31], mean squared error [29, 23, 3], supervised contrastive loss [5] and also for focal loss and label smoothing [30]. Recent works have spent efforts to extend the UFM to deeper architectures to study the behavior of more layers after the “unconstrained feature”. Specifically, [23] extends UFM to account for one additional layer, from one-layer linear classifier to two-layer linear classifier after the “unconstrained” features for MSE loss, and later the work [3] extends the setting to a general deep linear network for both MSE and CE losses. [23] also extends UFM for MSE loss to a two-layer case with ReLU activation. This setting is later extended by [21] to the general deep UFM with ReLU activation for the binary classification problem. There are efforts to mitigate the

restriction of UFM, such as [24] analyzes UFM with an additional regularization term to force the features to stay in the vicinity of a predefined feature matrix (e.g., intermediate features). Additionally, [31, 29, 30] further show the benign optimization landscape for several loss functions under the UFM setting, demonstrating that critical points can only be global minima or strict saddle points.

Neural Collapse on imbalanced dataset: The work [4] is likely the first to observe that for imbalanced setting, the collapse of features within the same class $\mathcal{NC1}$ is preserved, but the geometry skews away from ETF. They also present the "Minority Collapse" phenomenon, in which the minority classifiers collapse to the same vector if the imbalance level is greater than some threshold. For MSE loss, [3] has explicitly characterized the geometry of the learned features and classifiers for imbalanced setting. [3] shows that the $\mathcal{NC1}$ still holds and the class-means converge to a General Orthonormal Frame (GOF), which consists of orthonormal vectors but with different lengths. By applying non-negative constraints for the *normalized features*, [15] finds the global minimizers of supervised contrastive loss and proves that the optimal features form an Orthogonal frame (OF) with equal length and orthogonal vectors, regardless of the imbalance level. [22] theoretically studies the UFM-SVM problem, whose global minima follow a more general geometry than the ETF, called "SELI". However, this work also makes clear that the unregularized version of CE loss only converges to KKT points of the SVM problem, which are not necessarily global minima. The result for UFM-SVM is later extended by the work [1] to consider several cross-entropy parameterizations.

Regarding CE loss, [25] studies the imbalanced setting but with fixed, unlearnable last-layer linear classifiers as a simplex ETF. They prove that no matter whether the data distribution is balanced or not among classes, the features will converge to a simplex ETF in the same direction as the fixed classifier. As mentioned in Section 1, the work [8] is closest to our work and [8] studies CE loss with UFM and the features can have negative entries. They prove that the within-class features will collapse ($\mathcal{NC1}$) and the *network output prediction vectors converge to a block structure* where each block corresponds with a group of classes that have the same amount of training instances. However, since the magnitude of prediction vectors and the ratio between each block within the structure are not yet covered, it is not possible to describe the geometry explicitly and quantify how the structure changes under different imbalance levels. Furthermore, the structure of the learned last-layer feature, the classifier weight ($\mathcal{NC2}$) and the relation between them ($\mathcal{NC3}$) have not been derived in [8]. Therefore, the norm, the norm ratio and the angle between the classifier weights and features are not considered.

3 Problem Setup

Training Neural Network with Cross-Entropy Loss: In this work we focus on neural network trained using the cross-entropy (CE) loss function on an imbalanced dataset. We consider the classification task with K classes. Let n_k denote the number of training samples in class k -th, and $N := \sum_{k=1}^K n_k$, the total number of training samples. A typical deep neural network classifier consists of a feature mapping function $\mathbf{h}(\mathbf{x})$ and a linear classifier parameterized as \mathbf{W} . Specifically, a L -layer deep neural network can be expressed as follows:

$$\psi_{\mathbf{W},\theta}(\mathbf{x}) = \underbrace{\mathbf{W}}_{\text{Last-layer linear classifier } \mathbf{W}_L=\mathbf{W}} \underbrace{\sigma(\mathbf{W}_{L-1} \dots \sigma(\mathbf{W}_1 \mathbf{x} + \mathbf{b}_1) + \mathbf{b}_{L-1})}_{\text{Feature } \mathbf{h}=\mathbf{h}(\mathbf{x})}, \quad (1)$$

where each layer composes of an affine transformation parameterized by a weight matrix \mathbf{W}_l and bias \mathbf{b}_l , followed by a non-linear activation σ (e.g., $\text{ReLU}(x) = \max(x, 0)$). Here, $\boldsymbol{\theta} := \{\mathbf{W}_l, \mathbf{b}_l\}_{l=1}^L$ is the set of all learnable parameters in the feature mapping. Current paradigm trains the network by minimizing the empirical risk over all training samples $\{(\mathbf{x}_{k,i}, \mathbf{y}_k)\}_{k,i}$ where $\mathbf{x}_{k,i}$ denoted the i -th sample of class k and \mathbf{y}_k is the one-hot label vector for class k :

$$\min_{\mathbf{W}, \boldsymbol{\theta}} \frac{1}{N} \sum_{k=1}^K \sum_{i=1}^{n_k} \mathcal{L}(\psi_{\mathbf{W}, \boldsymbol{\theta}}(\mathbf{x}_{k,i}), \mathbf{y}_k) + \frac{\lambda_W}{2} \|\mathbf{W}\|_F^2 + \frac{\lambda_\theta}{2} \|\boldsymbol{\theta}\|^2, \quad (2)$$

where $\lambda_W, \lambda_\theta > 0$ are the weight decay parameters and $\mathcal{L}(\psi(\mathbf{x}_{k,i}), \mathbf{y}_k)$ is the loss function that measures the difference between the output $\psi(\mathbf{x}_{k,i})$ and the target \mathbf{y}_k . For a vector $\mathbf{z} = [z_1, z_2, \dots, z_K] \in \mathbb{R}^K$ and a target one-hot vector \mathbf{y}_k , CE loss is defined as:

$$\mathcal{L}_{CE}(\mathbf{z}, \mathbf{y}_k) = -\log \left(\frac{\exp(z_k)}{\sum_{m=1}^K \exp(z_m)} \right) \quad (3)$$

Unconstrained Feature Model (UFM) with non-negative features: Due to the significant challenges of analyzing the highly non-convex neural network training problem, a series of recent theoretical works study \mathcal{NC} phenomenon using a simplified model called unconstrained feature model (UFM), or, layer-peeled model [4]. In particular, UFM peels down the last-layer of the network and treats the last-layer features $\mathbf{h}_{k,i} = \mathbf{h}(\mathbf{x}_{k,i}) \in \mathbb{R}^d$ as free optimization variables in order to capture the main characteristics of the last layers related to \mathcal{NC} during training. This relaxation can be justified by the well-known result that an overparameterized deep neural network can approximate any continuous function [10, 9, 28, 26].

In this work, we consider a slight variant of UFM, in which the features are constrained to be non-negative. This is motivated by the fact that features are usually the output of ReLU activations in many common architectures. Formally, we consider the following modified version of UFM trained with CE loss with non-negative features:

$$\begin{aligned} \min_{\mathbf{W}, \mathbf{H}} \frac{1}{N} \sum_{k=1}^K \sum_{i=1}^{n_k} \mathcal{L}_{CE}(\mathbf{W}\mathbf{h}_{k,i}, \mathbf{y}_k) + \frac{\lambda_W}{2} \|\mathbf{W}\|_F^2 + \frac{\lambda_H}{2} \|\mathbf{H}\|_F^2, \\ \text{s.t. } \mathbf{H} \geq 0, \end{aligned} \quad (4)$$

where $\mathbf{H} := [\mathbf{h}_{1,1}, \dots, \mathbf{h}_{1,n_1}, \mathbf{h}_{2,1}, \dots, \mathbf{h}_{K,n_K}] \in \mathbb{R}^{d \times N}$ and $\mathbf{H} \geq 0$ denotes entry-wise non-negativity. We note that similar settings with ReLU features were previously considered in [19], which derives \mathcal{NC} configuration for the label smoothing loss under balanced setting, and in [15], which studies the convergence geometry for supervised contrastive loss under imbalanced setting. We denote this setting as UFM₊, as [15], to differentiate it from the original UFM setting.

By denoting $\mathbf{W} = [\mathbf{w}_1, \mathbf{w}_2, \dots, \mathbf{w}_K]^\top \in \mathbb{R}^{K \times d}$ be the last-layer weight matrix, with $\mathbf{w}_k \in \mathbb{R}^d$ is the k -th row of \mathbf{W} , the CE loss can be written as:

$$\mathcal{L}_{CE}(\mathbf{W}\mathbf{h}_{k,i}, \mathbf{y}_k) = -\log \left(\frac{\exp(\mathbf{w}_k^\top \mathbf{h}_{k,i})}{\sum_{m=1}^K \exp(\mathbf{w}_m^\top \mathbf{h}_{k,i})} \right). \quad (5)$$

We also denote the class-mean of class k as $\mathbf{h}_k := n_k^{-1} \sum_{i=1}^{n_k} \mathbf{h}_{k,i}$ and the global mean $\mathbf{h}_G := N^{-1} \sum_{k=1}^K \sum_{i=1}^{n_k} \mathbf{h}_{k,i}$. The class-mean matrix is denoted as $\overline{\mathbf{H}} = [\mathbf{h}_1, \mathbf{h}_2, \dots, \mathbf{h}_K] \in \mathbb{R}^{d \times K}$.

Neural Collapse for balanced dataset: With the notations defined above, we recall the \mathcal{NC} properties in the balanced setting as follows

- ($\mathcal{NC1}$) **Variability collapse:** $\mathbf{h}_{k,i} = \mathbf{h}_k, \quad \forall k \in [K], i \in [n_k]$.
- ($\mathcal{NC2}$) **Convergence to simplex ETF:** $(\overline{\mathbf{H}} - \mathbf{h}_G \mathbf{1}_K^\top)^\top (\overline{\mathbf{H}} - \mathbf{h}_G \mathbf{1}_K^\top) \propto \mathbf{I}_K - \frac{1}{K} \mathbf{1}_K \mathbf{1}_K^\top$
- ($\mathcal{NC3}$) **Convergence to self-duality:** $\mathbf{W} \propto \overline{\mathbf{H}}^\top$

Orthogonal Frame and General Orthogonal Frame: Some previous results, such as [23, 19] derive that under balanced setting, the optimal class-means $\{\mathbf{h}_k\}$ form an *orthogonal frame (OF)*, i.e., $\overline{\mathbf{H}}^\top \overline{\mathbf{H}} \propto \mathbf{I}_K$. By centering the OF structure with its mean vector, we will receive a simplex ETF, thus this structure still follows ($\mathcal{NC2}$) property above. For MSE loss but under imbalanced scenario, [3] proves that the class-means $\{\mathbf{h}_k\}$ form an orthogonal structure consisting of pairwise orthogonal vectors but having different lengths. They termed this structure as *general orthogonal frame (GOF)*. We will use this notation for our results in Section 4.

Imbalanced dataset: We consider the general classification problem with K classes and the number of training samples of k -th class is n_k . This setting is more general than those in previous works, where only two different class sizes are considered, i.e., the majority classes of n_A training samples and the minority classes of n_B samples with the imbalance ratio $R := n_A/n_B > 1$ [4, 22].

4 Main Result: Global Structure of UFM₊ Cross-Entropy Imbalanced

In this section, we characterize the global solution (\mathbf{W}, \mathbf{H}) of the non-convex problem (4) and analyze its geometries. We prove that, irrespective of the label distribution, the optimal features will form an orthogonal structure in the non-negative orthant while the classifiers spread across the whole feature space with $\sum_{k=1}^K \mathbf{w}_k = \mathbf{0}$. For convenience, we define the following constants for every class $k \in [K]$:

$$\begin{aligned} \overline{M}_k &:= \log \left((K-1) \left(\frac{\sqrt{n_k}}{N \sqrt{\frac{K-1}{K}} \lambda_W \lambda_H} - 1 \right) \right), \\ M_k &:= \begin{cases} \overline{M}_k & \text{if } \overline{M}_k > 0 \\ 0 & \text{if } \overline{M}_k \leq 0 \text{ or } \overline{M}_k \text{ is undefined} \end{cases}, \quad \forall k \in [K]. \end{aligned} \quad (6)$$

Note that the inequality $M_k = \overline{M}_k > 0$ is equivalent to $\frac{N}{\sqrt{n_k}} \sqrt{\lambda_W \lambda_H} < \sqrt{\frac{K-1}{K}}$ and $M_k = 0$ when and only when $\frac{N}{\sqrt{n_k}} \sqrt{\lambda_W \lambda_H} \geq \sqrt{\frac{K-1}{K}}$. We state our main result in the following theorem.

Theorem 1 (Structure of UFM₊ Cross-Entropy Imbalanced minimizers). *Suppose $d \geq K$ and $\frac{N}{\sqrt{n_k}} \sqrt{\lambda_W \lambda_H} < \sqrt{\frac{K-1}{K}} \forall k \in [K]$, then any global minimizer (\mathbf{W}, \mathbf{H}) of the problem (4) obeys*

(a) *Within-class feature collapse:*

$$\forall k \in [K], \mathbf{h}_{k,i} = \mathbf{h}_{k,j}, \quad \forall i \neq j. \quad (7)$$

(b) *Class-mean orthogonality:*

$$\mathbf{h}_k^\top \mathbf{h}_l = 0, \quad \forall k \neq l. \quad (8)$$

(c) *Class-mean norm:*

$$\|\mathbf{h}_k\|^2 = \sqrt{\frac{K-1}{K} \frac{\lambda_W}{\lambda_H} \frac{1}{n_k}} M_k. \quad (M_k \text{ is defined in Eqn. (6)}) \quad (9)$$

(d) *Relation between the classifier and class-means:*

$$\mathbf{w}_k = \sqrt{\frac{1}{K(K-1)}} \sqrt{\frac{\lambda_H}{\lambda_W}} \left(K \sqrt{n_k} \mathbf{h}_k - \sum_{m=1}^K \sqrt{n_m} \mathbf{h}_m \right), \quad \forall k \in [K], \quad (10)$$

and $\sum_{k=1}^K \mathbf{w}_k = \mathbf{0}$.

(e) *Prediction vector of class k -th sample:*

$$\mathbf{z}_k^{(k)} = (\mathbf{W} \mathbf{h}_k)^{(k)} = \frac{K-1}{K} M_k, \quad (11)$$

$$\mathbf{z}_k^{(m)} = (\mathbf{W} \mathbf{h}_k)^{(m)} = -\frac{1}{K} M_k, \quad \forall m \neq k, \quad (12)$$

and $\sum_{m=1}^K \mathbf{z}_k^{(m)} = 0$.

If there is any $k \in [K]$ such that $\frac{N}{\sqrt{n_k}} \sqrt{\lambda_W \lambda_H} \geq \sqrt{\frac{K-1}{K}}$, then the k -th class-mean $\mathbf{h}_k = \mathbf{0}$ and all properties above are still hold.

We postpone the detailed proof until Section 7. We discuss the implications of Theorem 1 in the following paragraphs.

Optimal features form a General Orthogonal Frame: As we observe from Theorem 1, every global solution exhibits the $\mathcal{NC}1$, i.e., within-class features collapse to their class-mean. Under the nonnegativity constraint, the optimal features will form the general orthogonal frame (GOF), which consists of pairwise orthogonal vectors but with different lengths. This structure is similar to the geometry of the optimal features of the UFM MSE imbalanced minimizers [3]. However, the optimal classifier \mathbf{w}_k of problem (4) with CE loss does not form an orthogonal structure as in the case of MSE under imbalance as in [3] (see the following paragraph). For UFM₊ imbalanced with supervised contrastive loss and normalized features (i.e., $\|\mathbf{h}\| = 1$), it is observed that optimal \mathbf{H} also exhibits GOF structure but with equal length class-mean vectors, irrespective to the imbalanced level [15].

Classifier converges to scaled-and-centered class-means: Our results indicate that class k 's classifier, \mathbf{w}_k , is aligned to the scaled and centered class-mean \mathbf{h}_k , with scaling factor $\sqrt{n_k}$, i.e., $\mathbf{w}_k \propto K\sqrt{n_k}\mathbf{h}_k - \sum_{m=1}^K \sqrt{n_m}\mathbf{h}_m$. Note that the proportional scalar between \mathbf{w}_k and $K\sqrt{n_k}\mathbf{h}_k - \sum_{m=1}^K \sqrt{n_m}\mathbf{h}_m$ is identical across k 's. This property generalizes the $\mathcal{NC3}$ convergence to self-duality originally defined for Neural Collapse where under balanced dataset, $\{\mathbf{w}_k\}$ are perfectly matched with the centered class-means $\mathbf{w}_k \propto K\mathbf{h}_K - \sum_{m=1}^K \mathbf{h}_m$.

Logit matrix and Margin: Each column \mathbf{z}_k of the logit matrix $\mathbf{Z} = \mathbf{W}\mathbf{H}$ is of a factor of the vector $\mathbf{y}_k - \frac{1}{K}\mathbf{1}_k$, but the factors are different among classes. Thus, the optimal matrix $\mathbf{Z} = \mathbf{W}\mathbf{H}$ of the problem (4) is different from the SELI geometry defined in [22], which is the global structure of the UFM-SVM imbalanced problem. This further proves the result in [22] that SELI is not the optimal structure for the CE imbalanced problem for any finite regularization parameter $\lambda > 0$. In addition, the margin for any data point $\mathbf{x}_{k,i}$ from class k is:

$$q_{k,i}(\mathbf{W}, \mathbf{H}) = \mathbf{w}_k^\top \mathbf{h}_{k,i} - \max_{j \neq k} \mathbf{w}_j^\top \mathbf{h}_{k,i} = M_k. \quad (13)$$

We derive the results of Theorem 1 in the special case of balanced dataset.

Corollary 1 (Balanced dataset as a special case). *Under balanced setting where $n_1 = n_2 = \dots = n_K$, we have $\mathbf{W} \propto (\mathbf{H} - \mathbf{h}_G \mathbf{1}_K^\top)^\top$ and thus,*

$$\mathbf{H}^\top \mathbf{H} \propto \mathbf{I}_K, \quad (OF)$$

$$\mathbf{W}\mathbf{W}^\top \propto (\mathbf{H} - \mathbf{h}_G \mathbf{1}_K^\top)^\top (\mathbf{H} - \mathbf{h}_G \mathbf{1}_K^\top) \propto \mathbf{I}_K - \frac{1}{K} \mathbf{1}_K \mathbf{1}_K^\top, \quad (ETF)$$

$$\mathbf{Z} = \mathbf{W}\mathbf{H} \propto (\mathbf{H} - \mathbf{h}_G \mathbf{1}_K^\top)^\top \mathbf{H} \propto \mathbf{I}_K - \frac{1}{K} \mathbf{1}_K \mathbf{1}_K^\top. \quad (ETF)$$

Proof. The results are directly obtained from Theorem 1 and by noting that $M_1 = M_2 = \dots = M_K$. When \mathbf{H} forms an OF, the center class-mean matrix $\mathbf{H} - \mathbf{h}_G \mathbf{1}_K^\top$ is a simplex ETF. This follows from

$$\begin{aligned} (\mathbf{H} - \mathbf{h}_G \mathbf{1}_K^\top)^\top (\mathbf{H} - \mathbf{h}_G \mathbf{1}_K^\top) &= (\mathbf{I}_K - \frac{1}{K} \mathbf{1}_K \mathbf{1}_K^\top)^\top \mathbf{H}^\top \mathbf{H} (\mathbf{I}_K - \frac{1}{K} \mathbf{1}_K \mathbf{1}_K^\top) \\ &\propto (\mathbf{I}_K - \frac{1}{K} \mathbf{1}_K \mathbf{1}_K^\top)^\top \mathbf{I}_K (\mathbf{I}_K - \frac{1}{K} \mathbf{1}_K \mathbf{1}_K^\top) \\ &= \mathbf{I}_K - \frac{1}{K} \mathbf{1}_K \mathbf{1}_K^\top. \end{aligned}$$

The logit matrix \mathbf{Z} also forms an ETF structure because

$$\mathbf{Z} = \mathbf{W}\mathbf{H} \propto (\mathbf{H} - \mathbf{h}_G \mathbf{1}_K^\top)^\top \mathbf{H} = (\mathbf{I}_K - \frac{1}{K} \mathbf{1}_K \mathbf{1}_K^\top)^\top \mathbf{H}^\top \mathbf{H} = \mathbf{I}_K - \frac{1}{K} \mathbf{1}_K \mathbf{1}_K^\top.$$

We obtain the conclusion of Corollary 1. □

For the special case where dataset is balanced, Theorem 1 recovers the ETF structure for classifier matrix \mathbf{W} and logit matrix \mathbf{Z} . The optimal class-mean matrix forms an OF since it is constrained to be on non-negative orthant.

4.1 Classifier Norm and Angle

By expressing the geometry of the optimal solutions explicitly, Theorem 1 allows us to derive closed-form expressions for the norms and angles between any individual classifiers and features. Under imbalanced regime, the k -th class classifier $\mathbf{w}_k \propto K\sqrt{n_k}\mathbf{h}_k - \sum_{m=1}^K \sqrt{n_m}\mathbf{h}_m$, indicating that its norm and the cosine of the angle formed with other classifier weights are negatively correlated with the number of sample n_k . We study the norm and angle of the classifier in the following proposition.

Proposition 1 (Classifiers norm and angle). *The optimal classifiers $\{\mathbf{w}_k\}_{k=1}^K$ of problem (4) obey:*

$$\begin{aligned} \|\mathbf{w}_k\|^2 &= \frac{1}{K\sqrt{K(K-1)}} \sqrt{\frac{\lambda_H}{\lambda_W}} \left((K-1)^2 \sqrt{n_k} M_k + \sum_{m \neq k} \sqrt{n_m} M_m \right), \\ \mathbf{w}_k^\top \mathbf{w}_j &= \frac{1}{K\sqrt{K(K-1)}} \sqrt{\frac{\lambda_H}{\lambda_W}} \left[-(K-1)\sqrt{n_k} M_k - (K-1)\sqrt{n_j} M_j + \sum_{m \neq k, j} \sqrt{n_m} M_m \right], k \neq j \\ \cos(\mathbf{w}_k, \mathbf{w}_j) &= \frac{\mathbf{w}_k^\top \mathbf{w}_j}{\|\mathbf{w}_k\| \|\mathbf{w}_j\|} \\ &= \frac{-(K-1)\sqrt{n_k} M_k - (K-1)\sqrt{n_j} M_j + \sum_{m \neq k, j} \sqrt{n_m} M_m}{\sqrt{((K-1)^2 \sqrt{n_k} M_k + \sum_{m \neq k} \sqrt{n_m} M_m)((K-1)^2 \sqrt{n_j} M_j + \sum_{m \neq j} \sqrt{n_m} M_m)}}, k \neq j. \end{aligned}$$

The fact that the weight norm is positively correlated with the number of training instances has been studied in the literature [13, 11, 14]. Our result in Proposition 1 is in agreement with this observation. It is also clear that under balanced scenario where $n_1 = n_2 = \dots = n_K$, the cosine of two classifier weight vector is equal $-1/(K-1)$, i.e., the pairwise angle of the simplex ETF. We proceed to derive the norm ratio of the classifier weight and class-means and the angles of the classifiers when we will have only two group of classes with equal number of samples in each group.

Corollary 2 (Norm ratios). *Suppose $d \geq K$ and (\mathbf{W}, \mathbf{H}) is a global minimizer of problem (4). Then, for any $i, j \in [K]$, we have*

$$\begin{aligned} \frac{\|\mathbf{w}_i\|^2}{\|\mathbf{w}_j\|^2} &= \frac{(K-1)^2 \sqrt{n_i} M_i + \sum_{m \neq i} \sqrt{n_m} M_m}{(K-1)^2 \sqrt{n_j} M_j + \sum_{m \neq j} \sqrt{n_m} M_m} \\ \frac{\|\mathbf{h}_i\|^2}{\|\mathbf{h}_j\|^2} &= \sqrt{\frac{n_j}{n_i} \frac{M_i}{M_j}} \end{aligned} \quad (14)$$

As a consequence, if $n_i \geq n_j$, $\|\mathbf{w}_i\| \geq \|\mathbf{w}_j\|$.

Proof. The results are direct consequences of Proposition 1. \square

For the norm of the optimal features, one might expect it is negatively correlated with the number of training samples and the results for UFM-MSE and UFM-SVM training problem agree with this expectation [3, 22]. However, for CE loss, we find that this statement is not always true because the function $M_i/\sqrt{n_i}$ is not always a decreasing function with respect to n_i .

Corollary 3 (Classifier angles). *Assume the dataset has K_A majority classes with n_A samples per class and K_B minority classes with n_B samples per class, then*

$$\cos(\mathbf{w}_{major}, \mathbf{w}'_{major}) = 1 - \frac{K^2 \sqrt{n_A} M_A}{K^2 \sqrt{n_A} M_A - K \sqrt{n_A} M_A - K_B \sqrt{n_A} M_A + K_B \sqrt{n_B} M_B}, \quad (15)$$

$$\cos(\mathbf{w}_{minor}, \mathbf{w}'_{minor}) = 1 - \frac{K^2 \sqrt{n_B} M_B}{K^2 \sqrt{n_B} M_B - K \sqrt{n_B} M_B - K_A \sqrt{n_B} M_B + K_A \sqrt{n_A} M_A}. \quad (16)$$

Consequently, we have $\cos(\mathbf{w}_{major}, \mathbf{w}'_{major}) < \cos(\mathbf{w}_{minor}, \mathbf{w}'_{minor})$.

Proof. The results are direct consequences of Proposition 1. \square

From Corollary 3, we deduce that the angle between classifier of major classes will form larger angles than those of minor classes. Additionally, since Eqn. (15) and (16) are true for any pair of classes of the same category, this means that classifiers of classes with the same number of training instances have the *same pairwise angle*.

4.2 Heavy Imbalances Cause Minority Collapse and Complete Collapse

Data naturally exhibit imbalance in their class distribution. The model trained on highly-skewed class distribution data tends to be biased the majority classes and having poor performance on the minority classes [11, 13, 14]. Especially, [4] observes that when the imbalance ratio $R := \frac{n_{major}}{n_{minor}}$ is larger than some threshold, the angle between minority classifiers become zero and these classifiers have about the same length. Thus, these classifiers become indistinguishable and the network would predict the same probabilities for these minor classes. This phenomenon is termed as Minority Collapse. From Theorem 1, we obtain the exact threshold of the Minority Collapse occurrence for every class in terms of the number of training samples and regularization parameters.

Corollary 4 (Minority Collapse and Complete Collapse). *For any class $k \in [K]$, if $n_k \leq C(N, K, \lambda_W, \lambda_H) := N^2 \frac{K}{K-1} \lambda_W \lambda_H$, then at the optimal solution of problem (4), $\mathbf{h}_k = 0$ and $\mathbf{w}_k = \mathbf{w}_{k'}$ for any $k' \in [K]$ such that $n_{k'} \leq C(N, K, \lambda_W, \lambda_H)$.*

- (a) *Minority Collapse: If the dataset has K_A majority classes with n_A samples per class and K_B minority classes with n_B samples per class, then Minority Collapse happens if the imbalance ratio*

$$R := \frac{n_A}{n_B} \geq \frac{1}{K_A} \left(\frac{K-1}{NK\lambda_W\lambda_H} - K_B \right), \quad (17)$$

with $K = K_A + K_B$ and $N = n_A K_A + n_B K_B$.

- (b) *Complete Collapse: If*

$$\frac{N^2}{n_A} \geq \frac{K-1}{K\lambda_W\lambda_H}, \quad (18)$$

then all classes collapse and the optimal solution is trivial, i.e., $(\mathbf{W}, \mathbf{H}) = (\mathbf{0}, \mathbf{0})$.

Proof. The results are direct consequences of Theorem 1. \square

Corollary 4 implies that even the head classes will collapse when the ratio N^2/n_A is large enough, i.e., the dataset has a huge amount of samples or has too many classes. The bound (18) suggests that we should lower the regularization level to avoid this *complete collapse* phenomenon.

5 Experimental Results

5.1 Metric definition

We recall the notation $\mathbf{h}_k := \frac{1}{n} \sum_{i=1}^n \mathbf{h}_{k,i}$, i.e., the class-means of class k and $\mathbf{h}_G := \frac{1}{K} \sum_{k=1}^K \sum_{i=1}^n \mathbf{h}_{k,i}$ is the feature global-mean. We calculate the within-class covariance matrix $\Sigma_W := \frac{1}{N} \sum_{k=1}^K \sum_{i=1}^n (\mathbf{h}_{k,i} - \mathbf{h}_k)(\mathbf{h}_{k,i} - \mathbf{h}_k)^\top$ and the between-class covariance matrix $\Sigma_B := \frac{1}{K} \sum_{k=1}^K (\mathbf{h}_k - \mathbf{h}_G)(\mathbf{h}_k - \mathbf{h}_G)^\top$.

Feature collapse. Following previous works [6, 31, 23], we measure feature collapse using $\mathcal{NC}1$ metric

$$\mathcal{NC}1 := \frac{1}{K} \text{trace}(\Sigma_W \Sigma_B^\dagger), \text{ where } \Sigma_B^\dagger \text{ is the Moore-Penrose inverse of } \Sigma_B. \quad (19)$$

Relation between the learned classifier \mathbf{W} and learned features \mathbf{H} . To verify the relation in Eqn.(10) in Theorem 1, we measure the similarity between the learned classifier \mathbf{W} and the UFM₊ structure described as follows

$$\mathcal{NC}2 := \left\| \frac{\mathbf{W}}{\|\mathbf{W}\|_F} - \frac{\mathbf{W}_{\text{UFM}_+}(\mathbf{H})}{\|\mathbf{W}_{\text{UFM}_+}(\mathbf{H})\|_F} \right\|_F, \text{ where } \mathbf{W}_{\text{UFM}_+}(\mathbf{H}) = \begin{bmatrix} K\sqrt{n_1}\mathbf{h}_1^\top - \sum_{m=1}^K \sqrt{n_m}\mathbf{h}_m^\top \\ K\sqrt{n_2}\mathbf{h}_2^\top - \sum_{m=1}^K \sqrt{n_m}\mathbf{h}_m^\top \\ \dots \\ K\sqrt{n_K}\mathbf{h}_K^\top - \sum_{m=1}^K \sqrt{n_m}\mathbf{h}_m^\top \end{bmatrix} \quad (20)$$

Prediction matrix \mathbf{WH} . To measure the similarity of the learned $\mathbf{Z} = \mathbf{WH}$ to the UFM₊ structure described in Theorem 1, we define $\mathcal{NC}3$ metric as follows

$$\mathcal{NC}3 := \left\| \frac{\mathbf{WH}}{\|\mathbf{WH}\|_F} - \frac{\mathbf{WH}_{\text{UFM}_+}}{\|\mathbf{WH}_{\text{UFM}_+}\|_F} \right\|_F, \text{ where } \mathbf{WH}_{\text{UFM}_+} = \begin{bmatrix} \frac{K-1}{K}M_1 & \frac{-1}{K}M_2 & \dots & \frac{-1}{K}M_K \\ \frac{-1}{K}M_1 & \frac{K-1}{K}M_2 & \dots & \frac{-1}{K}M_K \\ \dots & \dots & \dots & \dots \\ \frac{-1}{K}M_1 & \frac{-1}{K}M_2 & \dots & \frac{K-1}{K}M_K \end{bmatrix} \quad (21)$$

5.2 Experiment details

To verify our theoretical results, we perform experiments to mimic the UFM with ReLU features setting as in Eqn.(4). In particular, we use a 6-layer multilayer perceptron (MLP) model with ReLU activation and a ResNet18 [7] model as our two backbone feature extractors. We measure the evolution of three \mathcal{NC} metrics defined in Section 5.1 across training epochs and we also plot the matrices $\mathbf{H}^\top \mathbf{H}$ and \mathbf{WH} to demonstrate their orthogonal and block structure (respectively) at the end of training process.

We first discuss the training details. All experiments are performed on imbalanced subset of CIFAR10 [16] dataset for image classification task. To create the imbalanced training subset, we randomly sample each class from the original training set with number of training samples from the list [100, 100, 200, 200, 300, 300, 400, 400, 500, 500]. Each model is then trained with CE loss using stochastic gradient descent (SGD) for 4000 epochs, batch size 32. The learning rate is set to be divided

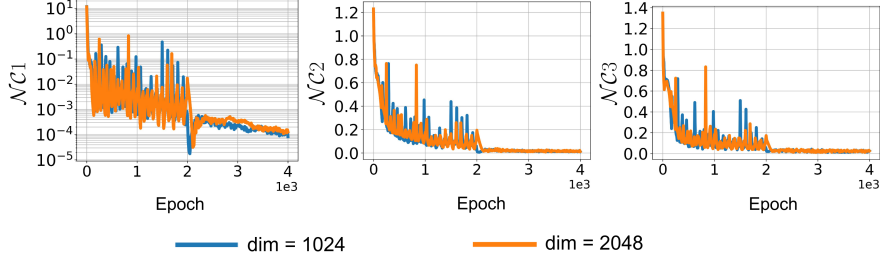


Figure 1: Illustration of $\mathcal{N}\mathcal{C}$ metrics for MLP trained on imbalanced subset of CIFAR10 dataset with cross entropy loss, and bias-free classifier \mathbf{W} .

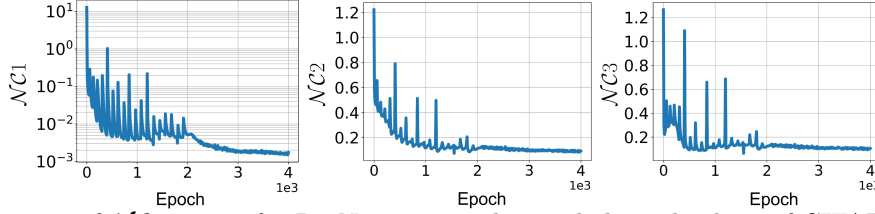


Figure 2: Illustration of $\mathcal{N}\mathcal{C}$ metrics for ResNet18 trained on imbalanced subset of CIFAR10 dataset with cross entropy loss, and bias-free classifier \mathbf{W} .

by 10 at 2000-th epoch. Feature decay rate is $\lambda_H = 1 \times 10^{-5}$ and weight decay rate is $\lambda_W = 1 \times 10^{-4}$.

MLP experiment: We use the 6-layer MLP backbone with hidden dimension $\in \{1024, 2048\}$ and the learning rates of 1×10^{-4} and 5×10^{-5} , respectively. Figure 1 demonstrate that as training progresses, $\mathcal{N}\mathcal{C}$ metrics converge to 0, which corroborates Theorem 1.

ResNet18 experiment: In ResNet18 experiment, we set learning rate to be 1×10^{-4} . Figure 2 shows that all $\mathcal{N}\mathcal{C}$ metrics also converges to small values in the end of training.

Illustration of $\mathbf{H}^\top \mathbf{H}$: We normalize the $\mathbf{H}^\top \mathbf{H}$ matrix from the last epoch of the trained MLP model with hidden dimension = 1024. The orthogonal structure of the learned features are demonstrated via Figure 3.

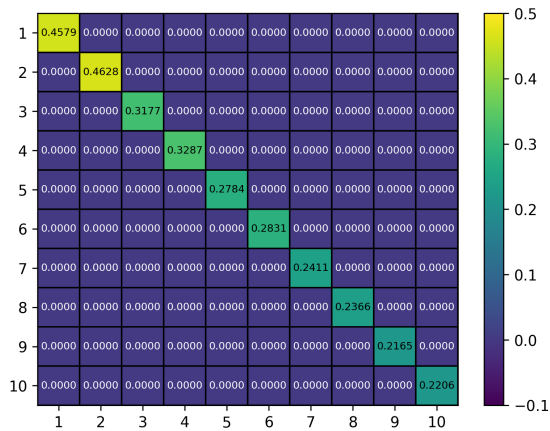


Figure 3: $\mathbf{H}^\top \mathbf{H}$ matrix extracted from the last epoch of the trained MLP model.

6 Concluding Remarks

In this work, we present a rigorous and explicit study of Neural Collapse phenomenon in the setting of imbalanced dataset using unconstrained non-negative feature model and cross-entropy loss. In particular, we provide a closed-form characterization of the last-layer features and classifier weights learned by the network training. We find that while the variability collapse property still holds, the geometry of the learned features and learned classifier weights are different from the original definition of Neural Collapse, due to the class-imbalance of the training data. Specifically, we prove that at optimality, the features form an orthogonal structure while the classifier weights are aligned to the scaled and centered class-means, which generalizes the original definition of Neural Collapse in class-balanced settings. Furthermore, with closed-form derivations of the solution, we are able to quantify the norms and the angles between the learned features and classifier weights across class distribution. As a limitation, we only study the convergence geometries under the condition that the feature dimension d is at least the number of classes K . The geometric structure of the features and classifier in the bottle-neck situation $d < K$ is still unknown and we leave it for future work.

7 Proof of Theorem 1 and Proposition 1

Recall the training problem:

$$\min_{\mathbf{W}, \mathbf{H}} \mathcal{L}_0(\mathbf{W}, \mathbf{H}) := \frac{1}{N} \sum_{k=1}^K \sum_{i=1}^{n_k} \mathcal{L}_{CE}(\mathbf{W}\mathbf{h}_{k,i}, \mathbf{y}_k) + \frac{\lambda_W}{2} \|\mathbf{W}\|_F^2 + \frac{\lambda_H}{2} \|\mathbf{H}\|_F^2, \quad (22)$$

where $\mathbf{h}_{k,i} \geq 0 \forall k, i$ and:

$$\mathcal{L}_{CE}(\mathbf{z}, \mathbf{y}_k) := -\log \left(\frac{e^{z_k}}{\sum_{i=1}^K e^{z_i}} \right).$$

Denoting the class-mean of k -th class as $\mathbf{h}_k = \frac{1}{n_k} \sum_{i=1}^{n_k} \mathbf{h}_{k,i}$, the m -th row vector of \mathbf{W} as \mathbf{w}_m . We denote $\mathbf{z}_{k,i} := \mathbf{W}\mathbf{h}_{k,i}$ and $\mathbf{z}^{(m)}$ is the m -th component of vector \mathbf{z} .

Step 1: We introduce a lower bound on the loss \mathcal{L}_0 by grouping the cross-entropy term and regularization term for features within the same class.

We have:

$$\begin{aligned}
\mathcal{L}_0(\mathbf{W}, \mathbf{H}) &= \frac{1}{N} \sum_{k=1}^K \sum_{i=1}^{n_k} \mathcal{L}_{CE}(\mathbf{z}_{k,i}, \mathbf{y}_k) + \frac{\lambda_W}{2} \|\mathbf{W}\|_F^2 + \frac{\lambda_H}{2} \|\mathbf{H}\|_F^2 \\
&= \frac{1}{N} \sum_{k=1}^K \left(\sum_{i=1}^{n_k} \log \left(\frac{\sum_{m=1}^K \exp(\mathbf{z}_{k,i}^{(m)})}{\exp(\mathbf{z}_{k,i}^{(k)})} \right) \right) + \frac{\lambda_W}{2} \|\mathbf{W}\|_F^2 + \frac{\lambda_H}{2} \sum_{k=1}^K \left(\sum_{i=1}^{n_k} \|\mathbf{h}_{k,i}\|^2 \right) \\
&= \frac{1}{N} \sum_{k=1}^K \left(\sum_{i=1}^{n_k} \log \left(1 + \sum_{m \neq k} \exp(\mathbf{z}_{k,i}^{(m)} - \mathbf{z}_{k,i}^{(k)}) \right) \right) + \frac{\lambda_W}{2} \|\mathbf{W}\|_F^2 + \frac{\lambda_H}{2} \sum_{k=1}^K \left(\sum_{i=1}^{n_k} \|\mathbf{h}_{k,i}\|^2 \right) \\
&\geq \frac{1}{N} \sum_{k=1}^K \left(\sum_{i=1}^{n_k} \log \left(1 + (K-1) \exp \left(\sum_{m \neq k} \frac{\mathbf{z}_{k,i}^{(m)} - \mathbf{z}_{k,i}^{(k)}}{K-1} \right) \right) \right) + \frac{\lambda_W}{2} \|\mathbf{W}\|_F^2 + \frac{\lambda_H}{2} \sum_{k=1}^K \left(\sum_{i=1}^{n_k} \|\mathbf{h}_{k,i}\|^2 \right) \\
&= \frac{1}{N} \sum_{k=1}^K \left(\sum_{i=1}^{n_k} \log \left(1 + (K-1) \exp \left(\frac{\sum_{m=1}^K \mathbf{z}_{k,i}^{(m)} - K \mathbf{z}_{k,i}^{(k)}}{K-1} \right) \right) \right) + \frac{\lambda_W}{2} \|\mathbf{W}\|_F^2 + \frac{\lambda_H}{2} \sum_{k=1}^K \left(\sum_{i=1}^{n_k} \|\mathbf{h}_{k,i}\|^2 \right) \\
&\geq \frac{1}{N} \sum_{k=1}^K n_k \log \left(1 + (K-1) \exp \left(\frac{1}{n_k} \sum_{i=1}^{n_k} \frac{\sum_{m=1}^K \mathbf{z}_{k,i}^{(m)} - K \mathbf{z}_{k,i}^{(k)}}{K-1} \right) \right) + \frac{\lambda_W}{2} \|\mathbf{W}\|_F^2 + \frac{\lambda_H}{2} \sum_{k=1}^K \left(\frac{1}{n_k} \left\| \sum_{i=1}^{n_k} \mathbf{h}_{k,i} \right\|^2 \right) \\
&= \frac{1}{N} \sum_{k=1}^K n_k \log \left(1 + (K-1) \exp \left(\frac{\sum_{m=1}^K \mathbf{z}_k^{(m)} - K \mathbf{z}_k^{(k)}}{K-1} \right) \right) + \frac{\lambda_W}{2} \|\mathbf{W}\|_F^2 + \frac{\lambda_H}{2} \sum_{k=1}^K n_k \|\mathbf{h}_k\|^2 \\
&= \frac{1}{N} \sum_{k=1}^K n_k \log \left(1 + (K-1) \exp \left(\frac{\sum_{m=1}^K \mathbf{w}_m \mathbf{h}_k - K \mathbf{w}_k \mathbf{h}_k}{K-1} \right) \right) + \frac{\lambda_W}{2} \|\mathbf{W}\|_F^2 + \frac{\lambda_H}{2} \sum_{k=1}^K n_k \|\mathbf{h}_k\|^2 \\
&:= \mathcal{L}_1(\mathbf{W}, \mathbf{H})
\end{aligned}$$

where $\mathbf{z}_k := \frac{1}{n_k} \sum_{i=1}^{n_k} \mathbf{z}_{k,i}$. We denote the function:

$$g(\mathbf{W}\mathbf{H}) := \frac{1}{N} \sum_{k=1}^K n_k \log \left(1 + (K-1) \exp \left(\frac{\sum_{m=1}^K \mathbf{w}_m \mathbf{h}_k - K \mathbf{w}_k \mathbf{h}_k}{K-1} \right) \right), \quad (23)$$

thus, $\mathcal{L}_1(\mathbf{W}, \mathbf{H}) = g(\mathbf{W}\mathbf{H}) + \frac{\lambda_W}{2} \|\mathbf{W}\|_F^2 + \frac{\lambda_H}{2} \sum_{k=1}^K n_k \|\mathbf{h}_k\|^2$.

The first inequality above follows from Jensen inequality that:

$$\sum_{m \neq k} \exp(\mathbf{z}_{k,i}^{(m)} - \mathbf{z}_{k,i}^{(k)}) \geq (K-1) \exp \left(\sum_{m \neq k} \frac{\mathbf{z}_{k,i}^{(m)} - \mathbf{z}_{k,i}^{(k)}}{K-1} \right), \quad (24)$$

which become equality when and only when $\mathbf{z}_{k,i}^{(m)} = \mathbf{z}_{k,i}^{(l)} \forall m, l \neq k$. The second inequality include two inequalities as following:

$$\sum_{i=1}^{n_k} \log \left(1 + (K-1) \exp \left(\frac{\sum_{m=1}^K \mathbf{z}_{k,i}^{(m)} - K \mathbf{z}_{k,i}^{(k)}}{K-1} \right) \right) \geq n_k \log \left(1 + (K-1) \exp \left(\frac{1}{n_k} \sum_{i=1}^{n_k} \frac{\sum_{m=1}^K \mathbf{z}_{k,i}^{(m)} - K \mathbf{z}_{k,i}^{(k)}}{K-1} \right) \right), \quad (25)$$

where we use Jensen inequality since the function $\log(1 + (K - 1) \exp(x))$ is a convex function. The second sub-inequality is that for any $k \in [K]$, $\sum_{i=1}^{n_k} \|\mathbf{h}_{k,i}\|^2 \geq \frac{1}{n_k} \|\sum_{k=1}^K \mathbf{h}_{k,i}\|^2$, which achieves equality if and only if $\mathbf{h}_{k,i} = \mathbf{h}_{k,j} \forall i \neq j$. This equality condition also satisfy the equality condition of the inequality (25), hence we only need to satisfy this property to achieve equality.

Step 2: We further lower bound the log term of \mathcal{L}_1 , the idea of this bound is inspired from Lemma D.5 in [31]

For any $k \in [K]$ and any $t_k > 0$, we have:

$$\begin{aligned}
& \log \left(1 + (K - 1) \exp \left(\frac{\sum_{m=1}^K \mathbf{z}_k^{(m)} - K \mathbf{z}_k^{(k)}}{K - 1} \right) \right) \\
&= \log \left(\frac{t_k}{1 + t_k} \frac{1 + t_k}{t_k} + \frac{1}{1 + t_k} (1 + t_k) (K - 1) \exp \left(\frac{\sum_{m=1}^K \mathbf{z}_k^{(m)} - K \mathbf{z}_k^{(k)}}{K - 1} \right) \right) \\
&\geq \frac{1}{1 + t_k} \log \left((1 + t_k) (K - 1) \exp \left(\frac{\sum_{m=1}^K \mathbf{z}_k^{(m)} - K \mathbf{z}_k^{(k)}}{K - 1} \right) \right) + \frac{t_k}{1 + t_k} \log \left(\frac{1 + t_k}{t_k} \right) \\
&= \frac{1}{1 + t_k} \frac{\sum_{m=1}^K \mathbf{z}_k^{(m)} - K \mathbf{z}_k^{(k)}}{K - 1} + \frac{1}{1 + t_k} \log \left((1 + t_k) (K - 1) \right) + \frac{t_k}{1 + t_k} \log \left(\frac{1 + t_k}{t_k} \right) \\
&= \underbrace{\frac{\sqrt{n_k}}{1 + t_k} \sqrt{\frac{1}{n_k} \sum_{m=1}^K \mathbf{z}_k^{(m)} - K \mathbf{z}_k^{(k)}}}_{c_{1,k}} + \underbrace{\frac{1}{1 + t_k} \log \left((1 + t_k) (K - 1) \right) + \frac{t_k}{1 + t_k} \log \left(\frac{1 + t_k}{t_k} \right)}_{c_{2,k}} \\
&= \frac{c_{1,k}}{K - 1} \frac{\sum_{m=1}^K \mathbf{z}_k^{(m)} - K \mathbf{z}_k^{(k)}}{\sqrt{n_k}} + c_{2,k},
\end{aligned} \tag{26}$$

where the inequality above is from the concavity of the $\log(x)$ function, i.e., $\log(tx + (1 - t)y) \geq t \log(x) + (1 - t) \log(y)$ for any x, y and $t \in [0, 1]$. The inequality becomes an equality if any only if:

$$\frac{1 + t_k}{t_k} = (1 + t_k) (K - 1) \exp \left(\frac{\sum_{m=1}^K \mathbf{z}_k^{(m)} - K \mathbf{z}_k^{(k)}}{K - 1} \right) \quad \text{or} \quad t_k = 0, \quad \text{or} \quad t_k = +\infty.$$

However, when $t_k = 0$ or $t_k = +\infty$, the equality is trivial. Therefore, we have:

$$t_k = \left[(K - 1) \exp \left(\frac{\sum_{m=1}^K \mathbf{z}_k^{(m)} - K \mathbf{z}_k^{(k)}}{K - 1} \right) \right]^{-1}.$$

To summary, at this step, we have that for any $k \in [K]$ and any $t_k > 0$:

$$\log \left(1 + (K - 1) \exp \left(\frac{\sum_{m=1}^K \mathbf{z}_k^{(m)} - K \mathbf{z}_k^{(k)}}{K - 1} \right) \right) \geq \frac{c_{1,k}}{K - 1} \frac{\sum_{m=1}^K \mathbf{z}_k^{(m)} - K \mathbf{z}_k^{(k)}}{\sqrt{n_k}} + c_{2,k}, \tag{27}$$

where $c_{1,k} = \sqrt{n_k}/(1 + t_k)$ and $c_{2,k} = \frac{1}{1 + t_k} \log \left((1 + t_k) (K - 1) \right) + \frac{t_k}{1 + t_k} \log \left(\frac{1 + t_k}{t_k} \right)$. The inequality becomes an equality when:

$$t_k = \left[(K - 1) \exp \left(\frac{\sum_{m=1}^K \mathbf{z}_k^{(m)} - K \mathbf{z}_k^{(k)}}{K - 1} \right) \right]^{-1} \tag{28}$$

Step 3: We apply the result from **Step 2** and choose the same $c_{1,k}$ for all classes to lower bound $g(\mathbf{WH})$ w.r.t. the L2-norm of the class-mean $\|\mathbf{h}_k\|^2 := x_k$.

By using the inequality (27) for $\mathbf{z}_{k,i} = \mathbf{W}\mathbf{h}_{k,i}$ and choosing the same scalar $c_1 := c_{1,1} = \dots = c_{1,k}$ (recall that $c_{1,k}$ can be chosen arbitrarily), we have:

$$\begin{aligned}
& \frac{K-1}{c_1} \left[g(\mathbf{WH}) - \sum_{k=1}^K \frac{n_k}{N} c_{2,k} \right] \\
&= \frac{K-1}{c_1} \left[\frac{1}{N} \sum_{k=1}^K n_k \log \left(1 + (K-1) \exp \left(\frac{\sum_{m=1}^K \mathbf{w}_m \mathbf{h}_k - K \mathbf{w}_k \mathbf{h}_k}{K-1} \right) \right) - \sum_{k=1}^K \frac{n_k}{N} c_{2,k} \right] \\
&\geq \frac{1}{N} \sum_{k=1}^K n_k \sqrt{\frac{1}{n_k}} \left[\sum_{m=1}^K \mathbf{w}_m \mathbf{h}_k - K \mathbf{w}_k \mathbf{h}_k \right] \\
&= \frac{1}{N} \sum_{m=1}^K \mathbf{w}_m \left(\sum_{k=1}^K \sqrt{n_k} \mathbf{h}_k - K \sqrt{n_m} \mathbf{h}_m \right)
\end{aligned} \tag{29}$$

We know that from the Cauchy-Schwarz inequality for inner product that for any $\mathbf{u}, \mathbf{v} \in \mathbb{R}^K$ and any $c_3 > 0$,

$$\mathbf{u}^\top \mathbf{v} \geq -\frac{c_3}{2} \|\mathbf{u}\|_2^2 - \frac{1}{2c_3} \|\mathbf{v}\|_2^2.$$

The equality holds when $c_3 \mathbf{u} = -\mathbf{v}$. Therefore, by applying this inequality for each term $\mathbf{w}_m \left(\sum_{k=1}^K \sqrt{n_k} \mathbf{h}_k - K \sqrt{n_m} \mathbf{h}_m \right)$, we have:

$$\begin{aligned}
& \frac{N(K-1)}{c_1} \left[g(\mathbf{WH}) - \sum_{k=1}^K \frac{n_k}{N} c_{2,k} \right] \\
&\geq -\frac{c_3}{2} \sum_{m=1}^K \|\mathbf{w}_m\|_2^2 - \frac{1}{2c_3} \sum_{m=1}^K \left\| \sum_{k=1}^K \sqrt{n_k} \mathbf{h}_k - K \sqrt{n_m} \mathbf{h}_m \right\|_2^2 \\
&= -\frac{c_3}{2} \|\mathbf{W}\|_F^2 - \frac{1}{2c_3} \sum_{m=1}^K \|\hat{\mathbf{h}}_m\|_2^2,
\end{aligned} \tag{30}$$

where we denote $\hat{\mathbf{h}}_m := \sum_{k=1}^K \sqrt{n_k} \mathbf{h}_k - K \sqrt{n_m} \mathbf{h}_m, \forall m \in [K]$, and the above inequality becomes an equality if and only if:

$$c_3 \mathbf{w}_m = - \sum_{k=1}^K \sqrt{n_k} \mathbf{h}_k + K \sqrt{n_m} \mathbf{h}_m, \forall m \in [K] \tag{31}$$

We further have:

$$\begin{aligned}
\sum_{m=1}^K \|\hat{\mathbf{h}}_m\|^2 &= \sum_{m=1}^K \left\| \sum_{k=1}^K \sqrt{n_k} \mathbf{h}_k - K \sqrt{n_m} \mathbf{h}_m \right\|^2 \\
&= \sum_{m=1}^K \left(\left\| \sum_{k=1}^K \sqrt{n_k} \mathbf{h}_k \right\|^2 + K^2 \|\sqrt{n_m} \mathbf{h}_m\|^2 - 2K \left\langle \sum_{k=1}^K \sqrt{n_k} \mathbf{h}_k, \sqrt{n_m} \mathbf{h}_m \right\rangle \right) \\
&= K^2 \sum_{m=1}^K \|\sqrt{n_m} \mathbf{h}_m\|^2 + K \left\| \sum_{k=1}^K \sqrt{n_k} \mathbf{h}_k \right\|^2 - 2K \left\langle \sum_{k=1}^K \sqrt{n_k} \mathbf{h}_k, \sum_{m=1}^K \sqrt{n_m} \mathbf{h}_m \right\rangle \\
&= K^2 \sum_{m=1}^K \|\sqrt{n_m} \mathbf{h}_m\|^2 - K \left\| \sum_{k=1}^K \sqrt{n_k} \mathbf{h}_k \right\|^2 \tag{32}
\end{aligned}$$

We lower bound the second term of Eqn. (32) as following:

$$\begin{aligned}
\left\| \sum_{k=1}^K \sqrt{n_k} \mathbf{h}_k \right\|^2 &= \sum_{k=1}^K \|\sqrt{n_k} \mathbf{h}_k\|^2 + \sum_{k,l,k \neq l} \langle \sqrt{n_k} \mathbf{h}_k, \sqrt{n_l} \mathbf{h}_l \rangle \\
&\geq \sum_{k=1}^K \|\sqrt{n_k} \mathbf{h}_k\|^2, \tag{33}
\end{aligned}$$

where we use the non-negativity of the features and the equality happens iff $\langle \mathbf{h}_k, \mathbf{h}_l \rangle = 0, \forall k \neq l$.

Thus, we have:

$$\sum_{m=1}^K \|\hat{\mathbf{h}}_m\|^2 \leq K(K-1) \sum_{k=1}^K n_k \|\mathbf{h}_k\|^2, \tag{34}$$

the equality happens iff $\langle \mathbf{h}_k, \mathbf{h}_l \rangle = 0, \forall k \neq l$.

Now, let $x_k := \|\mathbf{h}_k\|^2$, at critical points of \mathcal{L}_1 , from Lemma 1, we have:

$$\|\mathbf{W}\|_F^2 = \frac{\lambda_H}{\lambda_W} \sum_{k=1}^K n_k x_k. \tag{35}$$

Hence:

$$\frac{N(K-1)}{c_1} \left[g(\mathbf{W}\mathbf{H}) - \sum_{k=1}^K \frac{n_k}{N} c_{2,k} \right] \geq -\frac{c_3 \lambda_H}{2 \lambda_W} \left(\sum_{k=1}^K n_k x_k \right) - \frac{K(K-1)}{2c_3} \left(\sum_{k=1}^K n_k x_k \right) \tag{36}$$

We will choose c_3 in advance to let the inequality (36) hold. From the equality conditions (31) and (34), we can choose c_3 as follows:

$$\begin{aligned}
c_3 \mathbf{w}_m &= - \sum_{k=1}^K \sqrt{n_k} \mathbf{h}_k + K \sqrt{n_j} \mathbf{h}_m, \forall m \in [K] \\
\Rightarrow c_3^2 &= \frac{\sum_{k=1}^K \|\hat{\mathbf{h}}_k\|^2}{\sum_{k=1}^K \|\mathbf{w}_k\|^2} = \frac{K(K-1) \left(\sum_{k=1}^K n_k x_k \right)}{\frac{\lambda_H}{\lambda_W} \left(\sum_{k=1}^K n_k x_k \right)} = \frac{\lambda_W}{\lambda_H} K(K-1) \tag{37}
\end{aligned}$$

In summary, from (36), we have the lower bound of $g(\mathbf{WH})$:

$$g(\mathbf{WH}) \geq \frac{-c_1}{N} \sqrt{\frac{\lambda_H}{\lambda_W} \frac{K}{K-1}} \left(\sum_{k=1}^K n_k x_k \right) + \sum_{k=1}^K \frac{n_k}{N} c_{2,k}, \quad (38)$$

for any $c_1 > 0$. The equality conditions of (38) is derived at Lemma 2.

Step 4: Now, we use the lower bound of $g(\mathbf{WH})$ above into the bounding of the loss $\mathcal{L}_1(\mathbf{W}, \mathbf{H})$ and use the equality conditions from Lemma 2 to finish the bounding process.

Recall that $x_k = \|\mathbf{h}_k\|^2$, we have at critical points of \mathcal{L}_1 :

$$\begin{aligned} \mathcal{L}_1(\mathbf{W}, \mathbf{H}) &= g(\mathbf{WH}) + \frac{\lambda_W}{2} \|\mathbf{W}\|_F^2 + \frac{\lambda_H}{2} \sum_{k=1}^K n_k \|\mathbf{h}_k\|^2 \\ &\geq \frac{-c_1}{N} \sqrt{\frac{\lambda_H}{\lambda_W} \frac{K}{K-1}} \left(\sum_{k=1}^K n_k x_k \right) + \sum_{k=1}^K \frac{n_k}{N} c_{2,k} + \lambda_H \sum_{k=1}^K n_k x_k \\ &:= \xi(c_1, x_1, \dots, x_K), \end{aligned}$$

for any $c_1 > 0$ ($c_{2,k}$ can be calculated from c_1). From Lemma 2, we know that the inequality $\mathcal{L}_1(\mathbf{W}, \mathbf{H}) \geq \xi(c_1, x_1, \dots, x_K)$ becomes an equality if and only if:

$$\begin{aligned} \mathbf{h}_k^\top \mathbf{h}_l &= 0, \quad \forall k \neq l \\ \mathbf{w}_k &= \sqrt{\frac{1}{K(K-1)}} \sqrt{\frac{\lambda_H}{\lambda_W}} \left(K \sqrt{n_m} \mathbf{h}_m - \sum_{k=1}^K \sqrt{n_k} \mathbf{h}_k \right), \quad \forall k \in [K] \\ t_k &= \frac{1}{K-1} \exp \left(\sqrt{\frac{K}{K-1}} \sqrt{\frac{\lambda_H}{\lambda_W}} \sqrt{n_k} \|\mathbf{h}_k\|^2 \right), \\ c_1 &= \frac{\sqrt{n_k}}{1 + \frac{1}{K-1} \exp \left(\sqrt{\frac{K}{K-1}} \sqrt{\frac{\lambda_H}{\lambda_W}} \sqrt{n_k} \|\mathbf{h}_k\|^2 \right)} = \frac{\sqrt{n_l}}{1 + \frac{1}{K-1} \exp \left(\sqrt{\frac{K}{K-1}} \sqrt{\frac{\lambda_H}{\lambda_W}} \sqrt{n_l} \|\mathbf{h}_l\|^2 \right)}, \quad \forall k \neq l \end{aligned}$$

Next, we will lower bound $\xi(c_1, x_1, \dots, x_K)$ under these equality conditions for arbitrary values of x_1, \dots, x_K , as following:

$$\begin{aligned} &\xi(c_1, x_1, \dots, x_K) \\ &= \frac{-c_1}{N} \sqrt{\frac{\lambda_H}{\lambda_W} \frac{K}{K-1}} \left(\sum_{k=1}^K n_k x_k \right) + \sum_{k=1}^K \frac{n_k}{N} c_{2,k} + \lambda_H \sum_{k=1}^K n_k x_k \\ &= - \sum_{k=1}^K \frac{1}{N} \sqrt{\frac{\lambda_H}{\lambda_W} \frac{K}{K-1}} \frac{n_k \sqrt{n_k} x_k}{1+t_k} + \sum_{k=1}^K \frac{n_k}{N} \left(\frac{1}{1+t_k} \log((K-1)(1+t_k)) + \frac{t_k}{1+t_k} \log \left(\frac{1+t_k}{t_k} \right) \right) \\ &+ \lambda_H \sum_{k=1}^K n_k x_k. \end{aligned}$$

Due to the separation of the x_k 's, we can minimize them individually. Consider the following function, for any $k \in [K]$:

$$g(x) = -\frac{1}{N} \sqrt{\frac{\lambda_H}{\lambda_W} \frac{K}{K-1}} \frac{n_k \sqrt{n_k} x}{1+t} + \frac{n_k}{N} \left(\frac{1}{1+t} \log((K-1)(1+t)) + \frac{t}{1+t} \log\left(\frac{1+t}{t}\right) \right) + \lambda_H n_k x, \quad x \geq 0 \quad (39)$$

where $t = \frac{1}{K-1} \exp\left(\sqrt{\frac{K}{K-1}} \sqrt{\frac{\lambda_H}{\lambda_W}} \sqrt{n_k} x\right)$.

We note that:

$$\begin{aligned} & \frac{1}{1+t} \log((K-1)(1+t)) + \frac{t}{1+t} \log\left(\frac{1+t}{t}\right) \\ &= \frac{1}{1+t} \log((K-1)(1+t)) - \frac{1}{1+t} \log\left(\frac{1+t}{t}\right) + \log\left(\frac{1+t}{t}\right) \\ &= \frac{1}{1+t} \log((K-1)t) + \log\left(\frac{1+t}{t}\right) \\ &= \frac{\sqrt{\frac{\lambda_H}{\lambda_W} \frac{K}{K-1}} n_k x}{1+t} + \log\left(\frac{1+t}{t}\right). \end{aligned}$$

Hence:

$$g(x) = \frac{n_k}{N} \log\left(1 + (K-1) \exp\left(-\sqrt{\frac{K}{K-1}} \sqrt{\frac{\lambda_H}{\lambda_W}} \sqrt{n_k} x\right)\right) + \lambda_H n_k x$$

$$g'(x) = -\frac{n_k}{N} \frac{\sqrt{\frac{K}{K-1}} \sqrt{\frac{\lambda_H}{\lambda_W}} \sqrt{n_k}}{1 + \frac{1}{K-1} \exp\left(\sqrt{\frac{K}{K-1}} \sqrt{\frac{\lambda_H}{\lambda_W}} \sqrt{n_k} x\right)} + \lambda_H n_k \quad (40)$$

$$g'(x) = 0 \Rightarrow c_1 = \frac{\sqrt{n_k}}{1 + \frac{1}{K-1} \exp\left(\sqrt{\frac{K}{K-1}} \sqrt{\frac{\lambda_H}{\lambda_W}} \sqrt{n_k} x\right)} = N \sqrt{\frac{K-1}{K}} \lambda_W \lambda_H, \quad (41)$$

$$\Rightarrow x^* = \sqrt{\frac{K-1}{K} \frac{\lambda_W}{\lambda_H} \frac{1}{n_k}} \left(\log(K-1) + \log\left(\frac{\sqrt{n_k}}{N \sqrt{\frac{K-1}{K}} \lambda_W \lambda_H} - 1\right) \right). \quad (42)$$

Since $x = \|\mathbf{h}\|^2 \geq 0$, we have that $x^* > 0$ if $(K-1) \left(\frac{\sqrt{n_k}}{N \sqrt{\frac{K-1}{K}} \lambda_W \lambda_H} - 1\right) > 1$ or equivalently, $\frac{N}{\sqrt{n_k}} \sqrt{\lambda_W \lambda_H} < \sqrt{\frac{K-1}{K}}$. Otherwise, if $\frac{N}{\sqrt{n_k}} \sqrt{\lambda_W \lambda_H} \geq \sqrt{\frac{K-1}{K}}$, we have $g'(x) > 0 \quad \forall x > 0$ and thus, $x^* = 0$.

In conclusion, we have:

$$\mathcal{L}_1(\mathbf{W}, \mathbf{H}) = \xi(c_1, x_1, \dots, x_K) \geq \sum_{k=1}^K g(x_k^*) = \text{const}$$

For any (\mathbf{W}, \mathbf{H}) that the equality conditions at Lemma 2 do not hold, we have that $\mathcal{L}_1(\mathbf{W}, \mathbf{H}) > \xi \left(c_1 = N \sqrt{\frac{K-1}{K}} \lambda_W \lambda_H, x_1, \dots, x_K \right)$ and:

$$\begin{aligned}
& \xi \left(c_1 = N \sqrt{\frac{K-1}{K}} \lambda_W \lambda_H, x_1, \dots, x_K \right) \\
&= \frac{-c_1}{N} \sqrt{\frac{\lambda_H}{\lambda_W} \frac{K}{K-1}} \left(\sum_{k=1}^K n_k x_k \right) + \sum_{k=1}^K \frac{n_k}{N} c_{2,k} + \lambda_H \left(\sum_{k=1}^K n_k x_k \right) \\
&= \sum_{k=1}^K \frac{n_k}{N} c_{2,k} \\
&= \sum_{k=1}^K \frac{n_k}{N} \left(\frac{1}{1+t_k} \log((K-1)t_k) + \log \left(\frac{1+t_k}{t_k} \right) \right) \quad (\text{with } t_k = \sqrt{n_k}/c_1 - 1) \\
&= \sum_{k=1}^K g(x_k^*),
\end{aligned}$$

hence, (\mathbf{W}, \mathbf{H}) is not optimal.

Step 5: We finish the proof since $\mathcal{L}_0(\mathbf{W}, \mathbf{H}) \geq \mathcal{L}_1(\mathbf{W}, \mathbf{H}) \geq \text{const}$ and we study the equality conditions.

In conclusion, by summarizing all equality conditions, we have that any optimal $(\mathbf{W}^*, \mathbf{H}^*)$ of the original training problem obey the following:

- i) $\forall k \in [K], \mathbf{h}_{k,i} = \mathbf{h}_{k,j} \quad \forall i \neq j$
 - ii) $\mathbf{h}_k^\top \mathbf{h}_l = 0 \quad \forall k \neq l$
 - iii) $\mathbf{w}_k = \sqrt{\frac{1}{K(K-1)}} \sqrt{\frac{\lambda_H}{\lambda_W}} \left(K \sqrt{n_k} \mathbf{h}_k - \sum_{m=1}^K \sqrt{n_m} \mathbf{h}_m \right), \forall k \in [K]$
- and $\sum_{k=1}^K \mathbf{w}_k = \mathbf{0}$
- iv) $\|\mathbf{h}_k\|^2 = \sqrt{\frac{K-1}{K} \frac{\lambda_W}{\lambda_H} \frac{1}{n_k}} \log \left((K-1) \left(\frac{\sqrt{n_k}}{N \sqrt{\frac{K-1}{K}} \lambda_W \lambda_H} - 1 \right) \right)$
 - v) For $m \neq k, \mathbf{z}_k^{(m)} = (\mathbf{W} \mathbf{h}_k)^{(m)} = -\frac{1}{K} \log \left((K-1) \left(\frac{\sqrt{n_k}}{N \sqrt{\frac{K-1}{K}} \lambda_W \lambda_H} - 1 \right) \right),$
- $$\mathbf{z}_k^{(k)} = (\mathbf{W} \mathbf{h}_k)^{(k)} = \frac{K-1}{K} \log \left((K-1) \left(\frac{\sqrt{n_k}}{N \sqrt{\frac{K-1}{K}} \lambda_W \lambda_H} - 1 \right) \right)$$

We proceed to deduce the results of Proposition 1:

$$\begin{aligned}
\|\mathbf{w}_k\|^2 &= \frac{1}{K(K-1)} \frac{\lambda_H}{\lambda_W} \left\| (K-1)\sqrt{n_k}\mathbf{h}_k - \sum_{m \neq k} \sqrt{n_m}\mathbf{h}_m \right\|^2 \\
&= \frac{1}{K(K-1)} \frac{\lambda_H}{\lambda_W} \left((K-1)^2 n_k \|\mathbf{h}_k\|^2 + \sum_{m \neq k} n_m \|\mathbf{h}_m\|^2 \right) \\
&= \frac{1}{K\sqrt{K(K-1)}} \sqrt{\frac{\lambda_H}{\lambda_W}} \left((K-1)^2 \sqrt{n_k} M_k + \sum_{m \neq k} \sqrt{n_m} M_m \right), \\
\mathbf{w}_k^\top \mathbf{w}_j &= \frac{1}{K(K-1)} \frac{\lambda_H}{\lambda_W} \left\langle (K-1)\sqrt{n_k}\mathbf{h}_k - \sum_{m \neq k} \sqrt{n_m}\mathbf{h}_m, (K-1)\sqrt{n_j}\mathbf{h}_j - \sum_{m \neq j} \sqrt{n_m}\mathbf{h}_m \right\rangle \\
&= \frac{1}{K(K-1)} \frac{\lambda_H}{\lambda_W} \left(-(K-1)n_k \|\mathbf{h}_k\|^2 - (K-1)n_j \|\mathbf{h}_j\|^2 + \sum_{m \neq k, j} n_m \|\mathbf{h}_m\|^2 \right) \\
&= \frac{1}{K\sqrt{K(K-1)}} \sqrt{\frac{\lambda_H}{\lambda_W}} \left[-(K-1)\sqrt{n_k} M_k - (K-1)\sqrt{n_j} M_j + \sum_{m \neq k, j} \sqrt{n_m} M_m \right], k \neq j
\end{aligned}$$

7.1 Supporting lemmas

Remark: Although our training problem is a constrained optimization problem, the constraints $\mathbf{h}_{k,i} \geq 0$ are affine functions, it is clear that strong duality holds with dual variables equal 0's. Then, the solutions of the primal problem and the optimal dual variables will satisfy KKT conditions and hence, we have $\nabla_{\mathbf{H}} \mathcal{L}_1 = \mathbf{0}$ at optimal.

Lemma 1. Any critical points (\mathbf{W}, \mathbf{H}) of $\mathcal{L}_1(\mathbf{W}, \mathbf{H})$ satisfy:

$$\|\mathbf{W}\|_F^2 = \frac{\lambda_H}{\lambda_W} \sum_{k=1}^K n_k \|\mathbf{h}_k\|^2 \quad (43)$$

Proof of Lemma 1. Recall that $\mathcal{L}_1(\mathbf{W}, \mathbf{H}) = g(\mathbf{W}\mathbf{H}) + \frac{\lambda_W}{2} \|\mathbf{W}\|_F^2 + \frac{\lambda_H}{2} \sum_{k=1}^K n_k \|\mathbf{h}_k\|^2$. We have:

$$\begin{aligned}
\nabla_{\mathbf{W}} \mathcal{L}_1(\mathbf{W}, \mathbf{H}) &= \nabla_{\mathbf{Z}=\mathbf{W}\mathbf{H}} g(\mathbf{W}\mathbf{H}) \mathbf{H}^\top + \lambda_W \mathbf{W} = \mathbf{0} \\
\nabla_{\mathbf{H}} \mathcal{L}_1(\mathbf{W}, \mathbf{H}) &= \mathbf{W}^\top \nabla_{\mathbf{Z}=\mathbf{W}\mathbf{H}} g(\mathbf{W}\mathbf{H}) + \lambda_H [n_1 \mathbf{h}_1 \quad n_2 \mathbf{h}_2 \quad \dots \quad n_K \mathbf{h}_K] = \mathbf{0}
\end{aligned}$$

From $\mathbf{0} = \mathbf{W}^\top \nabla_{\mathbf{W}} \mathcal{L}_1(\mathbf{W}, \mathbf{H}) - \nabla_{\mathbf{H}} \mathcal{L}_1(\mathbf{W}, \mathbf{H}) \mathbf{H}^\top$, we have:

$$\lambda_W \mathbf{W}^\top \mathbf{W} = \lambda_H [n_1 \mathbf{h}_1 \quad n_2 \mathbf{h}_2 \quad \dots \quad n_K \mathbf{h}_K] \mathbf{H}^\top$$

Hence, by taking the trace of both sides, we have $\|\mathbf{W}\|_F^2 = \frac{\lambda_H}{\lambda_W} \sum_{k=1}^K n_k \|\mathbf{h}_k\|^2$. \square

Lemma 2. *The lower bound (38) is attained for any critical points (\mathbf{W}, \mathbf{H}) if and only if the following hold:*

$$\mathbf{h}_k^\top \mathbf{h}_l = 0, \forall k \neq l \quad (44)$$

$$\mathbf{w}_k = \sqrt{\frac{1}{K(K-1)}} \sqrt{\frac{\lambda_H}{\lambda_W}} \left(K\sqrt{n_m} \mathbf{h}_m - \sum_{k=1}^K \sqrt{n_k} \mathbf{h}_k \right), \forall k \in [K] \quad (45)$$

$$t_k = \frac{1}{K-1} \exp \left(\sqrt{\frac{K}{K-1}} \sqrt{\frac{\lambda_H}{\lambda_W}} \sqrt{n_k} \|\mathbf{h}_k\|^2 \right) \quad (46)$$

$$c_1 = \frac{\sqrt{n_k}}{1 + \frac{1}{K-1} \exp \left(\sqrt{\frac{K}{K-1}} \sqrt{\frac{\lambda_H}{\lambda_W}} \sqrt{n_k} \|\mathbf{h}_k\|^2 \right)} = \frac{\sqrt{n_l}}{1 + \frac{1}{K-1} \exp \left(\sqrt{\frac{K}{K-1}} \sqrt{\frac{\lambda_H}{\lambda_W}} \sqrt{n_l} \|\mathbf{h}_l\|^2 \right)}, \forall k \neq l \quad (47)$$

Proof of Lemma 2. From the proof above, we see that if we want to achieve the lower bound (36), we need that:

$$\mathbf{h}_k^\top \mathbf{h}_l = 0 \quad \forall k, l \in [K], k \neq l,$$

to achieve equality for the inequality (34).

We further need the following to obey (31):

$$\begin{aligned} c_3 \mathbf{w}_k &= - \left(\sum_{k=1}^K \sqrt{n_k} \mathbf{h}_k - K\sqrt{n_m} \mathbf{h}_m \right), \forall k \in [K] \quad \text{with } c_3 = \sqrt{\frac{\lambda_W}{\lambda_H} K(K-1)} \\ \Rightarrow \mathbf{w}_k &= \sqrt{\frac{1}{K(K-1)}} \sqrt{\frac{\lambda_H}{\lambda_W}} \left(K\sqrt{n_m} \mathbf{h}_m - \sum_{k=1}^K \sqrt{n_k} \mathbf{h}_k \right), \forall k \in [K]. \end{aligned}$$

Thus:

$$\sum_{k=1}^K \mathbf{w}_k = \mathbf{0} \quad (48)$$

Next, we need the inequality (30) to hold. Equivalently, this means that the equality condition (28) need to hold. Indeed, for a given $k \in [K]$ and any $m \neq k$:

$$\begin{aligned} \mathbf{z}_k^{(m)} &= \mathbf{w}_m \mathbf{h}_k \\ &= \sqrt{\frac{1}{K(K-1)}} \sqrt{\frac{\lambda_H}{\lambda_W}} \left(K\sqrt{n_m} \mathbf{h}_m - \sum_{l=1}^K \sqrt{n_l} \mathbf{h}_l \right) \mathbf{h}_k \\ &= - \sqrt{\frac{1}{K(K-1)}} \sqrt{\frac{\lambda_H}{\lambda_W}} \sqrt{n_k} \|\mathbf{h}_k\|^2 \\ \Rightarrow \mathbf{z}_k^{(m)} &= \mathbf{z}_k^{(l)} \quad \forall m, l \neq k \end{aligned} \quad (49)$$

We further have, for any $k \in [K]$:

$$\begin{aligned}
\sum_{m=1}^K \mathbf{z}_k^{(m)} &= \left(\sum_{m=1}^K \mathbf{w}_m \right) \mathbf{h}_k = 0, \\
K \mathbf{z}_k^{(k)} &= K \mathbf{w}_k \mathbf{h}_k = K \sqrt{\frac{1}{K(K-1)}} \sqrt{\frac{\lambda_H}{\lambda_W}} \left(K \sqrt{n_k} \mathbf{h}_k - \sum_{m=1}^K \sqrt{n_m} \mathbf{h}_m \right) \mathbf{h}_k \\
&= \sqrt{K(K-1)} \sqrt{\frac{\lambda_H}{\lambda_W}} \sqrt{n_k} \|\mathbf{h}_k\|^2 \\
\Rightarrow t_k &= \left[(K-1) \exp \left(\frac{\sum_{m=1}^K \mathbf{z}_k^{(m)} - K \mathbf{z}_k^{(k)}}{K-1} \right) \right]^{-1} = \frac{1}{K-1} \exp \left(\sqrt{\frac{K}{K-1}} \sqrt{\frac{\lambda_H}{\lambda_W}} \sqrt{n_k} \|\mathbf{h}_k\|^2 \right)
\end{aligned} \tag{50}$$

Since the scalar c_1 is chosen to be the same for all $k \in [K]$, we have:

$$c_1 = \frac{\sqrt{n_k}}{1+t_k} = \frac{\sqrt{n_k}}{1 + \frac{1}{K-1} \exp \left(\sqrt{\frac{K}{K-1}} \sqrt{\frac{\lambda_H}{\lambda_W}} \sqrt{n_k} \|\mathbf{h}_k\|^2 \right)}, \forall k \in [K] \tag{51}$$

□

References

- [1] T. Behnia, G. R. Kini, V. Vakilian, and C. Thrampoulidis. On the implicit geometry of cross-entropy parameterizations for label-imbalanced data. In *International Conference on Artificial Intelligence and Statistics*, pages 10815–10838. PMLR, 2023. (Cited on pages 2, 3, and 4.)
- [2] K. Cao, C. Wei, A. Gaidon, N. Arechiga, and T. Ma. Learning imbalanced datasets with label-distribution-aware margin loss, 2019. (Cited on page 2.)
- [3] H. Dang, T. Nguyen, T. Tran, H. Tran, and N. Ho. Neural collapse in deep linear network: From balanced to imbalanced data. *arXiv preprint arXiv:2301.00437*, 2023. (Cited on pages 2, 3, 4, 6, 7, and 9.)
- [4] C. Fang, H. He, Q. Long, and W. J. Su. Exploring deep neural networks via layer-peeled model: Minority collapse in imbalanced training. *Proceedings of the National Academy of Sciences*, 118(43), oct 2021. (Cited on pages 2, 4, 5, 6, and 10.)
- [5] F. Graf, C. D. Hofer, M. Niethammer, and R. Kwitt. Dissecting supervised contrastive learning, 2023. (Cited on page 3.)
- [6] X. Y. Han, V. Papan, and D. L. Donoho. Neural collapse under mse loss: Proximity to and dynamics on the central path, 2021. (Cited on page 11.)
- [7] K. He, X. Zhang, S. Ren, and J. Sun. Deep residual learning for image recognition. In *2016 IEEE Conference on Computer Vision and Pattern Recognition, CVPR 2016, Las Vegas, NV, USA, June 27-30, 2016*, pages 770–778. IEEE Computer Society, 2016. (Cited on page 11.)

- [8] W. Hong and S. Ling. Neural collapse for unconstrained feature model under cross-entropy loss with imbalanced data. *arXiv preprint arXiv:2309.09725*, 2023. (Cited on pages 2, 3, and 4.)
- [9] K. Hornik. Approximation capabilities of multilayer feedforward networks. *Neural Networks*, 4(2):251–257, 1991. (Cited on page 5.)
- [10] K. Hornik, M. Stinchcombe, and H. White. Multilayer feedforward networks are universal approximators. *Neural Networks*, 2(5):359–366, 1989. (Cited on page 5.)
- [11] C. Huang, Y. Li, C. C. Loy, and X. Tang. Learning deep representation for imbalanced classification. In *Proceedings of the IEEE conference on computer vision and pattern recognition*, pages 5375–5384, 2016. (Cited on pages 9 and 10.)
- [12] B. Kang, Y. Li, S. Xie, Z. Yuan, and J. Feng. Exploring balanced feature spaces for representation learning. In *International Conference on Learning Representations*, 2020. (Cited on page 2.)
- [13] B. Kang, S. Xie, M. Rohrbach, Z. Yan, A. Gordo, J. Feng, and Y. Kalantidis. Decoupling representation and classifier for long-tailed recognition, 2019. (Cited on pages 2, 9, and 10.)
- [14] B. Kim and J. Kim. Adjusting decision boundary for class imbalanced learning. *IEEE Access*, 8:81674–81685, 2020. (Cited on pages 2, 9, and 10.)
- [15] G. R. Kini, V. Vakilian, T. Behnia, J. Gill, and C. Thrampoulidis. Supervised-contrastive loss learns orthogonal frames and batching matters. *arXiv preprint arXiv:2306.07960*, 2023. (Cited on pages 3, 4, 5, and 7.)
- [16] A. Krizhevsky, G. Hinton, et al. Learning multiple layers of features from tiny images, 2009. (Cited on page 11.)
- [17] X. Liu, J. Zhang, T. Hu, H. Cao, Y. Yao, and L. Pan. Inducing neural collapse in deep long-tailed learning. In *International Conference on Artificial Intelligence and Statistics*, pages 11534–11544. PMLR, 2023. (Cited on page 2.)
- [18] J. Lu and S. Steinerberger. Neural collapse with cross-entropy loss, 2020. (Cited on pages 2 and 3.)
- [19] D. A. Nguyen, R. Levie, J. Liene, E. Hüllermeier, and G. Kutyniok. Memorization-dilation: Modeling neural collapse under noise. In *The Eleventh International Conference on Learning Representations*, 2022. (Cited on pages 5 and 6.)
- [20] V. Pappas, X. Y. Han, and D. L. Donoho. Prevalence of neural collapse during the terminal phase of deep learning training. *CoRR*, abs/2008.08186, 2020. (Cited on page 2.)
- [21] P. Sůkeník, M. Mondelli, and C. Lampert. Deep neural collapse is provably optimal for the deep unconstrained features model. *arXiv preprint arXiv:2305.13165*, 2023. (Cited on page 3.)
- [22] C. Thrampoulidis, G. R. Kini, V. Vakilian, and T. Behnia. Imbalance trouble: Revisiting neural-collapse geometry, 2022. (Cited on pages 2, 3, 4, 6, 8, and 9.)
- [23] T. Tirer and J. Bruna. Extended unconstrained features model for exploring deep neural collapse, 2022. (Cited on pages 3, 6, and 11.)

- [24] T. Tirer, H. Huang, and J. Niles-Weed. Perturbation analysis of neural collapse. In *International Conference on Machine Learning*, pages 34301–34329. PMLR, 2023. (Cited on page 4.)
- [25] Y. Yang, S. Chen, X. Li, L. Xie, Z. Lin, and D. Tao. Inducing neural collapse in imbalanced learning: Do we really need a learnable classifier at the end of deep neural network?, 2022. (Cited on page 4.)
- [26] D. Yarotsky. Universal approximations of invariant maps by neural networks, 2018. (Cited on page 5.)
- [27] H.-J. Ye, H.-Y. Chen, D.-C. Zhan, and W.-L. Chao. Identifying and compensating for feature deviation in imbalanced deep learning. *arXiv preprint arXiv:2001.01385*, 2020. (Cited on page 2.)
- [28] D.-X. Zhou. Universality of deep convolutional neural networks, 2018. (Cited on page 5.)
- [29] J. Zhou, X. Li, T. Ding, C. You, Q. Qu, and Z. Zhu. On the optimization landscape of neural collapse under mse loss: Global optimality with unconstrained features, 2022. (Cited on pages 3 and 4.)
- [30] J. Zhou, C. You, X. Li, K. Liu, S. Liu, Q. Qu, and Z. Zhu. Are all losses created equal: A neural collapse perspective, 2022. (Cited on pages 3 and 4.)
- [31] Z. Zhu, T. Ding, J. Zhou, X. Li, C. You, J. Sulam, and Q. Qu. A geometric analysis of neural collapse with unconstrained features. *CoRR*, abs/2105.02375, 2021. (Cited on pages 2, 3, 4, 11, and 15.)